

# Second harmonic generation at 399 nm resonant on the $^1S_0 - ^1P_1$ transition of ytterbium using a periodically poled $\text{LiNbO}_3$ waveguide

Takumi Kobayashi,<sup>1\*</sup> Daisuke Akamatsu,<sup>1</sup> Yoshiki Nishida,<sup>2</sup> Takehiko Tanabe,<sup>1</sup> Masami Yasuda,<sup>1</sup> Feng-Lei Hong,<sup>3,1</sup> and Kazumoto Hosaka<sup>1</sup>

<sup>1</sup>National Metrology Institute of Japan (NMIJ), National Institute of Advanced Industrial Science and Technology (AIST), 1-1-1 Umezono, Tsukuba, Ibaraki 305-8563, Japan

<sup>2</sup>NTT Electronics Corporation, 6700-2 To, Naka-shi, Ibaraki 311-0122, Japan

<sup>3</sup>Department of Physics, Graduate School of Engineering, Yokohama National University, 79-5 Tokiwadai, Hodogaya-ku, Yokohama 240-8501, Japan

\*[takumi-kobayashi@aist.go.jp](mailto:takumi-kobayashi@aist.go.jp)

**Abstract:** We demonstrate a compact and robust method for generating a 399-nm light resonant on the  $^1S_0 - ^1P_1$  transition in ytterbium using a single-pass periodically poled  $\text{LiNbO}_3$  waveguide for second harmonic generation (SHG). The obtained output power at 399 nm was 25 mW when a 798-nm fundamental power of 380 mW was coupled to the waveguide. We observed no degradation of the SHG power for 13 hours with a low power of 6 mW. The obtained SHG light has been used as a seed light for injection locking, which provides sufficient power for laser cooling ytterbium.

© 2021 Optical Society of America

**OCIS codes:** (190.2620) Harmonic generation and mixing; (130.3730) Lithium niobate; (020.3320) Laser cooling; (130.7405) Wavelength conversion devices.

## References and links

1. T. Kohno, M. Yasuda, K. Hosaka, H. Inaba, Y. Nakajima, and F.-L. Hong, "One-dimensional optical lattice clock with a fermionic  $^{171}\text{Yb}$  isotope," *Appl. Phys. Express* **2**, 072501 (2009).
2. M. Yasuda, H. Inaba, T. Kohno, T. Tanabe, Y. Nakajima, K. Hosaka, D. Akamatsu, A. Onae, T. Suzuyama, M. Amemiya, and F.-L. Hong, "Improved absolute frequency measurement of the  $^{171}\text{Yb}$  optical lattice clock towards a candidate for the redefinition of the second," *Appl. Phys. Express* **5**, 102401 (2012).
3. C. Y. Park, D.-H. Yu, W.-K. Lee, S. E. Park, E. B. Kim, S. K. Lee, J. W. Cho, T. H. Yoon, J. Mun, S. J. Park, T. Y. Kwon, and S.-B. Lee, "Absolute frequency measurement of  $^1S_0(F=1/2) - ^3P_0(F=1/2)$  transition of  $^{171}\text{Yb}$  atoms in a one-dimensional optical lattice at KRISS," *Metrologia* **50**, 119-128 (2013).
4. N. Hinkley, J. A. Sherman, N. B. Phillips, M. Schioppo, N. D. Lemke, K. Beloy, M. Pizzocaro, C. W. Oates, and A. D. Ludlow, "An atomic clock with  $10^{-18}$  instability," *Science* **341**, 1215-1218 (2013).
5. S. Sugawa, K. Inaba, S. Taie, R. Yamazaki, M. Yamashita, and Y. Takahashi, "Interaction and filling-induced quantum phases of dual Mott insulators of bosons and fermions," *Nat. Phys.* **7**, 642-648 (2011).
6. S. Taie, S. Sugawa, R. Yamazaki, and Y. Takahashi, "An  $\text{SU}(6)$  Mott insulator of an atomic Fermi gas realized by large-spin Pomeranchuk cooling," *Nat. Phys.* **8**, 825-830 (2012).
7. A. V. Gorshkov, A. M. Rey, A. J. Daley, M. M. Boyd, J. Ye, P. Zoller, and M. D. Lukin, "Alkali-earth-metal atoms as few-qubit quantum registers," *Phys. Rev. Lett.* **102**, 110503 (2009).
8. A. Daley, "Quantum computing and quantum simulation with group-II atoms," *Quantum Inf. Proc.* **10**, 865-884 (2011).
9. B. J. Bloom, T. L. Nicholson, J. R. Williams, S. L. Campbell, M. Bishof, X. Zhang, W. Zhang, S. L. Bromley, and J. Ye, "An optical lattice clock with accuracy and stability at the  $10^{-18}$  level," *Nature* **506**, 71-75 (2014).
10. I. Ushijima, M. Takamoto, M. Das, T. Ohkubo, and H. Katori, "Cryogenic optical lattice clocks," *Nat. Photonics* **6**, 185-189 (2015).

11. T. L. Nicholson, S. L. Campbell, R. B. Hutson, G. E. Marti, B. J. Bloom, R. L. McNally, W. Zhang, M. D. Barrett, M. S. Safronova, G. F. Strouse, W. L. Tew, and J. Ye, "Systematic evaluation of an atomic clock at  $2 \times 10^{-18}$  total uncertainty," *Nat. Commun.* **6**, 6896 (2015).
12. D. Akamatsu, M. Yasuda, H. Inaba, K. Hosaka, T. Tanabe, A. Onae, and F.-L. Hong, "Frequency ratio measurement of  $^{171}\text{Yb}$  and  $^{87}\text{Sr}$  optical lattice clocks," *Opt. Express* **22**, 7898-7905 (2014).
13. N. Nemitz, T. Ohkubo, M. Takamoto, I. Ushijima, M. Das, N. Ohmae, and H. Katori, "Frequency ratio of Yb and Sr clocks with  $5 \times 10^{-17}$  uncertainty at 150 s averaging time," *Nat. Photonics* doi:10.1038/nphoton.2016.20 (2016).
14. S. Blatt, A. D. Ludlow, G. K. Campbell, J. W. Thomsen, T. Zelevinsky, M. M. Boyd, J. Ye, X. Baillard, M. Fouché, R. Le Targat, A. Brusch, P. Lemonde, M. Takamoto, F.-L. Hong, H. Katori, and V. V. Flambaum, "New limits on coupling of fundamental constants to gravity using  $^{87}\text{Sr}$  optical lattice clocks," *Phys. Rev. Lett.* **100**, 140801 (2008).
15. T. Rosenband, D. B. Hume, P. O. Schmidt, C. W. Chou, A. Brusch, L. Lorini, W. H. Oskay, R. E. Drullinger, T. M. Fortier, J. E. Stalnaker, S. A. Diddams, W. C. Swann, N. R. Newbury, W. M. Itano, D. J. Wineland, and J. C. Bergquist, "Frequency ratio of  $\text{Al}^+$  and  $\text{Hg}^+$  single-ion optical clocks; metrology at the 17th decimal place," *Science* **319**, 1808-1812 (2008).
16. C. W. Chou, D. B. Hume, T. Rosenband, and D. J. Wineland, "Optical clocks and relativity," *Science* **329**, 1630-1633 (2010).
17. T. P. Krisher, "Gravitational redshift in a local freely falling frame: A proposed new null test of the equivalence principle," *Phys. Rev. D* **53**, R1735-R1739 (1996).
18. A. Derevianko and M. Pospelov, "Hunting for topological dark matter with atomic clocks," *Nat. Phys.* **10**, 933-936 (2014).
19. G. Mura, T. Franzen, C. A. Jaoudeh, A. Görlitz, H. Luckmann, I. Ernsting, A. Nevsky, S. Schiller, and the SOC2 Team, "A transportable optical lattice clock using  $^{171}\text{Yb}$ ," in *Joint European Frequency and Time Forum & International Frequency Control Symposium, EFTF/IFC 376-378* (2013).
20. N. Poli, M. Schioppo, S. Vogt, S. Falke, U. Sterr, C. Lisdat, and G. M. Tino, "A transportable strontium optical lattice clock," *Appl. Phys. B* **117**, 1107-1116 (2014).
21. K. Bongs, Y. Singh, L. Smith, W. He, O. Kock, D. Świerad, J. Hughes, S. Schiller, S. Alighanbari, S. Origlia, S. Vogt, U. Sterr, C. Lisdat, R. Le Targat, J. Lodewyck, D. Holleville, B. Venon, S. Bize, G. P. Barwood, P. Gill, I. R. Hill, Y. B. Ovchinnikov, N. Poli, G. M. Tino, J. Stuhler, and W. Kaenders, "Development of a strontium optical lattice clock for the SOC mission on the ISS," *C. R. Physique* **16**, 553-564 (2015).
22. J. I. Kim, C. Y. Park, J. Y. Yeom, E. B. Kim, and T. H. Yoon, "Frequency-stabilized high-power violet laser diode with an ytterbium hollow-cathode lamp," *Opt. Lett.* **28**, 245-247 (2003).
23. T. Kohno, M. Yasuda, H. Inaba, and F.-L. Hong, "Optical frequency stability measurement of an external cavity blue diode laser with an optical frequency comb," *Jpn. J. Appl. Phys.* **47**, 8856-8858 (2008).
24. K. Komori, Y. Takasu, M. Kumakura, Y. Takahashi, and T. Yabuzaki, "Injection-locking of blue laser diodes and its application to the laser cooling of neutral ytterbium atoms," *Jpn. J. Appl. Phys.* **42**, 5059-5062 (2003).
25. C. Y. Park and T. H. Yoon, "Frequency stabilization of injection-locked violet laser diode with Doppler-free absorption signal of ytterbium," *Jpn. J. Appl. Phys.* **42**, L754-L756 (2003).
26. T. Hosoya, M. Miranda, R. Inoue, and M. Kozuma, "Injection locking of a high power ultraviolet laser diode for laser cooling of ytterbium atoms," *Rev. Sci. Instrum.* **86**, 073110 (2015).
27. C. Adams and A. Ferguson, "Tunable narrow linewidth ultra-violet light generation by frequency doubling of a ring Ti:sapphire laser using lithium triborate in an external enhancement cavity," *Opt. Commun.* **90**, 89-94 (1992).
28. V. Ruseva, J. Hald, "Generation of UV light by frequency doubling in BIBO," *Opt. Commun.* **236**, 219-223 (2004).
29. F.-Y. Wang, B.-S. Shi, Q.-F. Chen, C. Zhai, G.-C. Guo, "Efficient cw violet-light generation in a ring cavity with a periodically poled KTP," *Opt. Commun.* **281**, 4114-4117 (2008).
30. Y. Onoda, M. Ikeda, K. Sugiyama, H. Yokoyama, and M. Kitano, "Maximization of second-harmonic power using normal-cut nonlinear crystals in a high-enhancement external cavity," *Appl. Opt.* **48**, 1366-1370 (2009).
31. M. Pizzocaro, D. Calonico, P. C. Pastor, J. Catani, G. A. Costanzo, F. Levi, and L. Lorini, "Efficient frequency doubling at 399 nm," *Appl. Opt.* **53**, 3388-3392 (2014).
32. X. Wen, Y. Han, J. Bai, J. He, Y. Wang, B. Yang, and J. Wang, "Cavity-enhanced frequency doubling from 795nm to 397.5nm ultra-violet coherent radiation with PPKTP crystals in the low pump power regime," *Opt. Express* **22**, 32293-32300 (2014).
33. Y. Han, X. Wen, J. Bai, B. Yang, Y. Wang, J. He, and J. Wang, "Generation of 130 mW of 397.5 nm tunable laser via ring-cavity-enhanced frequency doubling," *J. Opt. Soc. Am. B* **31**, 1942-1947 (2014).
34. X. Wen, Y. Han, and J. Wang, "Comparison and characterization of efficient frequency doubling at 397.5 nm with PPKTP, LBO and BiBO crystals," *Laser Phys.* **26**, 045401 (2016).
35. H. Jiang, G. Li, and X. Xu, "Highly efficient single-pass second harmonic generation in a periodically poled  $\text{MgO}:\text{LiNbO}_3$  waveguide pumped by a fiber laser at 1111.6 nm," *Opt. Express* **17**, 16073-16080 (2009).
36. S. Guo, J. Wang, Y. Han, and J. He, "Frequency doubling of cw 1560nm laser with single-pass, doubling-pass

- and cascaded MgO:PPLN crystals and frequency locking to Rb  $D_2$  line,” Proc. SPIE **8772**, 87721B (2013).
37. R. Bege, D. Jedrzejczyk, G. Blume, J. Hormann, D. Feise, K. Paschke, and G. Tränkle, “Watt-level second-harmonic generation at 589 nm with a PPMgO:LN ridge waveguide crystal pumped by a DBR tapered diode laser,” Opt. Lett. **41**, 1530-1533 (2016).
  38. T. Nishikawa, A. Ozawa, Y. Nishida, M. Asobe, F.-L. Hong, and T. W. Hänsch, “Efficient 494 mW sodium resonance radiation from sum-frequency generation by using a periodically poled Zn:LiNbO<sub>3</sub> ridge waveguide,” Opt. Express **17**, 17792-17800 (2009).
  39. D. Akamatsu, M. Yasuda, T. Kohno, A. Onae, and F.-L. Hong, “A compact light source at 461 nm using a periodically poled LiNbO<sub>3</sub> waveguide for strontium magneto-optical trapping,” Opt. Express **19**, 2046-2051 (2011).
  40. M. Asobe, O. Tadanaga, T. Yanagawa, H. Itoh, and H. Suzuki, “Reducing photorefractive effect in periodically poled ZnO- and MgO-doped LiNbO<sub>3</sub> wavelength converters,” Appl. Phys. Lett. **78**, 3163-3165 (2001).
  41. L. E. Myers, R. C. Eckardt, M. M. Fejer, R. L. Byer, W. R. Bosenberg, and J. W. Pierce, “Quasi-phase-matched optical parametric oscillators in bulk periodically poled LiNbO<sub>3</sub>,” J. Opt. Soc. Am. B **12**, 2102-2116 (1995).
  42. Y. Nishida, H. Miyazawa, M. Asobe, O. Tadanaga, and H. Suzuki, “Direct-bonded QPM-LN ridge waveguide with high damage resistance at room temperature,” Electron. Lett. **39** 609-611 (2003).
  43. K. R. Parameswaran, J. R. Kurz, R. V. Roussev, and M. M. Fejer, “Observation of 99% pump depletion in single-pass second-harmonic generation in a periodically poled lithium niobate waveguide,” Opt. Lett. **27**, 43-45 (2002).
  44. A. Yariv, *Optical Electronics in Modern Communications* (Oxford University, 1997).
  45. D. H. Jundt, “Temperature-dependent Sellmeier equation for the index of refraction,  $n_e$ , in congruent lithium niobate,” Opt. Lett. **22**, 1553-1555 (1997).
  46. I. Shoji, T. Kondo, A. Kitamoto, M. Shirane, and R. Ito, “Absolute scale of second-order nonlinear optical coefficients,” J. Opt. Soc. Am. B **14**, 2268-2294 (1997).
  47. K. Mizuuchi, A. Morikawa, T. Sugita, and K. Yamamoto, “Efficient second-harmonic generation of 340-nm light in a 1.4- $\mu$ m periodically poled bulk MgO:LiNbO<sub>3</sub>,” Jpn. J. Appl. Phys. **42**, L90-L91 (2003).
  48. A. Bouchier, G. Lucas-Leclin, P. Georges, and J. M. Maillard, “Frequency doubling of an efficient continuous wave single-mode Yb-doped fiber laser at 978 nm in a periodically-poled MgO:LiNbO<sub>3</sub> waveguide,” Opt. Express **13**, 6974-6979 (2005).
  49. M. Yasuda, T. Kohno, H. Inaba, Y. Nakajima, K. Hosaka, A. Onae, and F.-L. Hong, “Fiber-comb-stabilized light source at 556 nm for magneto-optical trapping of ytterbium,” J. Opt. Soc. Am. B **27**, 1388-1393 (2010).
  50. D. Akamatsu, Y. Nakajima, H. Inaba, K. Hosaka, M. Yasuda, A. Onae, and F.-L. Hong, “Narrow linewidth laser system realized by linewidth transfer using a fiber-based frequency comb for the magneto-optical trapping of strontium,” Opt. Express **20**, 16010-16016 (2012).
  51. H. Inaba, K. Hosaka, M. Yasuda, Y. Nakajima, K. Iwakuni, D. Akamatsu, S. Okubo, T. Kohno, A. Onae, and F.-L. Hong, “Spectroscopy of <sup>171</sup>Yb in an optical lattice based on laser linewidth transfer using a narrow linewidth frequency comb,” Opt. Express **21**, 7891-7896 (2013).

## 1. Introduction

Cold-atom experiments with ytterbium (Yb) atoms are of great interest in various research fields, including optical lattice clocks [1–4], quantum simulation [5, 6], and quantum information processing [7, 8]. Among these fields, optical lattice clocks have recently attracted considerable attention thanks to demonstrations of uncertainties at the  $10^{-18}$  level [9–11] and precise frequency ratio measurements of Yb and strontium (Sr) lattice clocks [12, 13]. Such accurate clocks are expected to contribute to the redefinition of the SI second, the search for time variations of fundamental physical constants [14, 15], relativistic geodesy [16], and other tests of fundamental physics [17, 18]. Some of these applications require robust transportable clocks. Several groups have therefore developed transportable optical lattice clocks [19–21].

In experiments with cold Yb atoms, high power light sources operating at 399 nm resonant on the  $^1S_0 - ^1P_1$  transition are used to cool atoms to a millikelvin temperature. A compact and robust 399-nm light source is essential for cold Yb experiments including development of a transportable Yb optical lattice clock. Several groups have employed blue external cavity diode lasers (ECDL) emitting at 399 nm [22, 23]. To obtain sufficient power for cooling Yb atoms, an injection locked 399-nm diode laser has usually been adopted to amplify the output power from a 399-nm ECDL [24–26]. Another approach to generating a 399-nm light has been to utilize the second harmonic generation (SHG) of a red laser operating at 798 nm, e.g., a 798-

nm ECLD. A 798-nm diode laser is useful for constructing an external cavity laser, since the laser has good longitudinal and transverse modes and is widely available. Conventionally, a nonlinear optical crystal, e.g., a lithium triborate (LBO), a barium borate (BBO), a  $\text{BiB}_3\text{O}_6$ , or a periodically poled  $\text{KTiOPO}_4$  crystal, has been placed in a power-buildup cavity to obtain a high SHG power [27–34]. The output power at 399 nm using this method is typically higher than that of the blue diode laser system. However, this SHG scheme requires the locking of a high-finesse cavity, which increases the number of stabilization parts and thus compromises the compactness and robustness of a laser system.

This paper presents the SHG of a 798-nm light using a single-pass periodically-poled  $\text{LiNbO}_3$  (PPLN) waveguide. High conversion efficiency in a single-pass configuration can be obtained with a PPLN waveguide, since its waveguide structure allows a tightly confined beam to propagate a long distance in a PPLN crystal [35–37]. A PPLN waveguide is therefore attractive for developing a compact and robust laser system at 399 nm. Our previous reports regarding a single-pass PPLN waveguide include the generation of a 589-nm light with a power of 494 mW [38] and a 461-nm light with a power of 76 mW [39]. In the present work, an output power of 25 mW is generated at 399 nm when a fundamental power of 380 mW is coupled to the PPLN waveguide. The output power of a blue light near 400 nm is generally low, since the wavelength is close to the edge of ultraviolet absorption in a PPLN crystal. The fundamental power at 798 nm can easily be obtained using a robust and conventional setup consisting of a 798-nm ECDL and a tapered amplifier. By using the generated 399-nm light as a seed light for injection locking, a power of more than 200 mW can be obtained [26], which is sufficient for cooling Yb atoms.

## 2. Experimental setup

Figure 1 is a schematic diagram of the experimental setup. To evaluate the PPLN waveguide, we employed a titanium sapphire (Ti:S) laser (M Squared, SolsTiS) operating at 798 nm as a fundamental input light source. The 798-nm beam was allowed to pass through a half-wave plate and coupled into a polarization-maintaining (PM) fiber. The half-wave plate was used to adjust the polarization direction to maximize the coupling efficiency into the PM fiber, and hence the SHG light power. The total coupling efficiency of the fundamental light into the PPLN waveguide including the fiber coupling was about 40%. The obtained SHG light was separated from the residual fundamental light using an interference filter. The PPLN waveguide was housed in a module package, a picture of which is shown in [38]. The temperature of the metal base of the PPLN waveguide was monitored with a thermistor and controlled at  $< 0.01$  °C with a Peltier device to meet the phase matching condition.

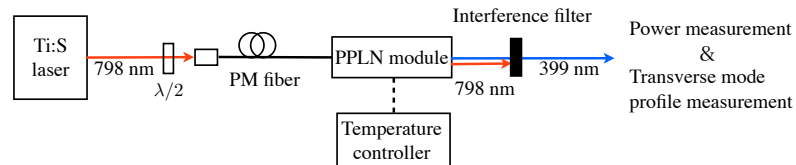


Fig. 1. Schematic diagram of the experimental setup. Ti:S: Titanium sapphire,  $\lambda/2$ : Half-wave plate, PM: Polarization-maintaining, PPLN: Periodically poled lithium niobate

The PPLN waveguide was manufactured by NTT Electronics Corp. A 3-inch diameter 5-mol% ZnO-doped LiNbO<sub>3</sub> wafer of which material is highly resistant to photorefractive damage [40] and a 3-inch diameter LiTaO<sub>3</sub> wafer whose refractive index is lower than that of LiNbO<sub>3</sub> were used for the waveguide layer and substrate, respectively. Two wafers were brought into contact with each other without using any adhesives and then annealed at 500 °C to achieve complete bonding. We used a conventional electrical poling method [41] to fabricate the periodically poled structure. Since there is a resolution limit for a photoresist pattern of narrower than 2 μm using contact lithography, 3rd-order quasi-phase matching with periodically poled period of 7.625 μm was realized in advance on the ZnO-doped LiNbO<sub>3</sub>. The waveguide layer thickness was reduced to 9.8 μm by successive lapping and polishing. We then fabricated a 11.6 μm-wide and 22 mm-long waveguide using a dicing saw [42].

### 3. Experimental results

Figure 2(a) shows the measured SHG power as a function of the coupled fundamental power. The power value was corrected for the loss at the interference filter. A maximum power of 25 mW was obtained at 399 nm when the coupled fundamental power was 380 mW. The experimental data were fitted with the following formula based on the pump depletion model [43],

$$P_{\text{out}}^{2\omega} = \eta P_{\text{in}}^{\omega} = P_{\text{in}}^{\omega} \tanh^2(\sqrt{\eta_0 P_{\text{in}}^{\omega}} L), \quad (1)$$

where  $P_{\text{out}}^{2\omega}$  denotes the output power of the SHG light,  $P_{\text{in}}^{\omega}$  the input power of the fundamental light,  $\eta$  the conversion efficiency, and  $L$  the waveguide length. The normalized nonlinear effi-

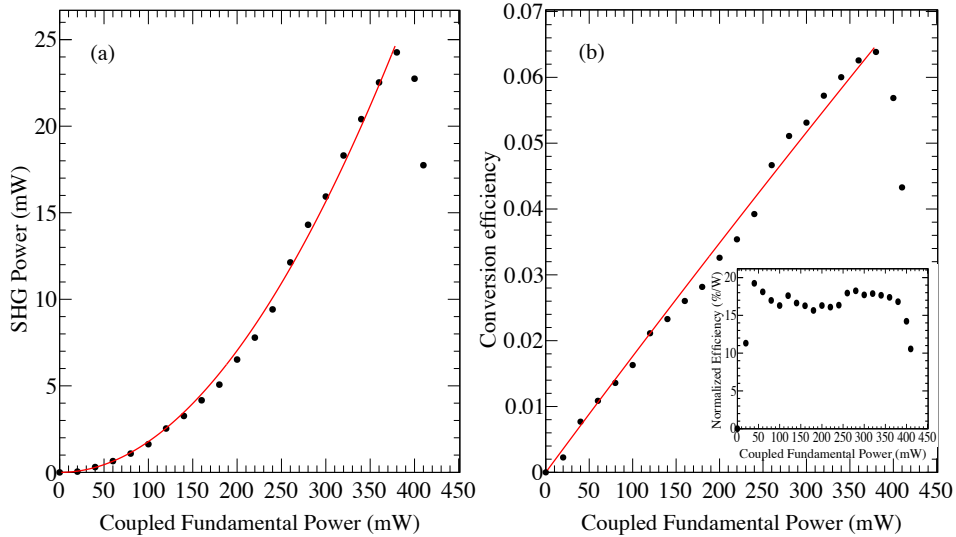


Fig. 2. SHG power (a) and conversion efficiency (b) as a function of the coupled fundamental power. The solid red curve indicates the best fit of a function based on the pump depletion model (see text). The inset in (b) shows the normalized conversion efficiency against the coupled fundamental power.

ciency  $\eta_0$  is proportional to the square of the effective nonlinear coefficient  $d_{\text{eff}}$  (see Sect. 4). The fitting result for  $P_{\text{in}}^{\omega} \leq 380$  mW is shown in Fig. 2(a) as a solid red line. The SHG power was found to decrease for  $P_{\text{in}}^{\omega} > 380$  mW. We believe this is due to the absorption of the 399-nm light in the PPLN waveguide. This gives rise to a temperature gradient along the waveguide, which cannot be compensated for by the spatially uniform temperature control. Figure 2(b) shows the conversion efficiency  $\eta$ , with the fitting for  $P_{\text{in}}^{\omega} \leq 380$  mW. The maximum conversion efficiency was 6.4% when the coupled fundamental power was 380 mW. The inset in Fig. 2(b) shows the normalized conversion efficiency  $\eta' = P_{\text{out}}^{2\omega} / (P_{\text{in}}^{\omega})^2$ . The normalized conversion efficiency was about 18%/W.

We measured the waveguide temperature dependence of the SHG power. When the fundamental power was 160 mW, the temperature acceptance bandwidth of the phase matching was  $\leq 0.5$  °C as shown in Fig. 3(a). The acceptance became narrower ( $< 0.1$  °C) for a high fundamental power of 400 mW as shown in Fig. 3(b). In this case, the waveguide temperature should be carefully controlled to obtain a stable SHG power. For example, the PPLN module package can be covered with a box to suppress temperature fluctuation [39]. The narrowing of the temperature acceptance is predicted by the pump depletion model [43] and has also been observed in our previous studies of a PPLN waveguide at 461 nm [39]. The temperature required to obtain the peak SHG power decreased by 2.6 °C when the fundamental power was changed from 160 to 400 mW. This was because of the absorption of the 399-nm light inside the PPLN waveguide.

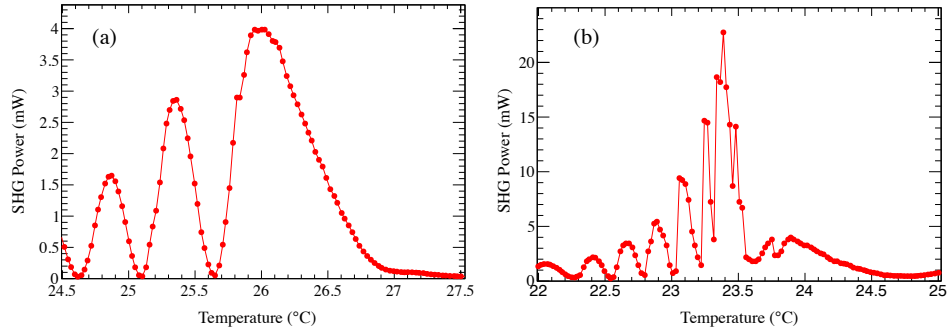


Fig. 3. Waveguide temperature dependence of the SHG power, where the coupled fundamental power is (a) 160 mW and (b) 400 mW.

The long-term stability of the SHG power was investigated in the low power region where the temperature acceptance is relatively broad. Figure 4 shows the SHG power as a function of time. The room temperature varied about  $\pm 1$  °C during the measurement. No degradation of the SHG power was observed for 13 hours until we switched off the laser. The SHG power fluctuation was less than 8%. This is considered to be due to the variation in the room temperature or the fluctuation of the coupling efficiency into the PM fiber. We also operated the PPLN module for several months and confirmed that the SHG power was stable day after day.

Figure 5 shows the transverse mode profile of the SHG output beam measured with a charge-coupled device camera. The profile was well-fitted by a Gaussian function. The ellipticity was 0.97. We confirmed that the coupling efficiency of the output beam into a single-mode fiber was

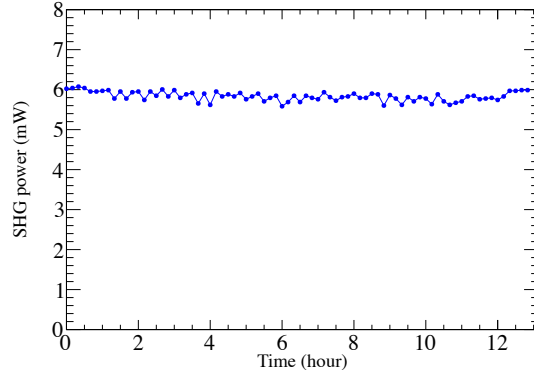


Fig. 4. Long-term stability of the SHG output power for a coupled fundamental power of 190 mW.

about 70%.

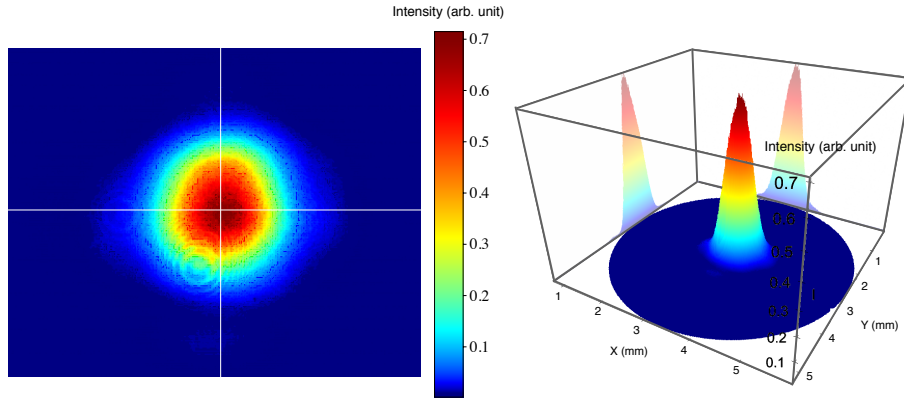


Fig. 5. Transverse mode profile of an SHG output beam.

#### 4. Discussion and conclusion

The nonlinear coefficient  $d_{\text{eff}}$  of the PPLN waveguide based on 3rd-order quasi-phase matching was calculated to be about 3 pm/V from the fitting parameter  $\eta_0$  (see Sect. 3) and the relationship,

$$d_{\text{eff}} = \frac{c}{\omega} \sqrt{\epsilon_0 c n(\omega) n(2\omega) S \sqrt{\eta_0}}, \quad (2)$$

where  $c$ ,  $\epsilon_0$ ,  $n(\omega)$ , and  $S$  are the speed of light, the vacuum permittivity, the refractive index of the waveguide for the fundamental frequency  $\omega$ , and the cross section of the waveguide, respectively [44]. In this calculation, the refractive indices  $n(\omega)$  and  $n(2\omega)$  were estimated using a Sellmeier equation with coefficients given in [45]. The calculated nonlinear coefficient of the present PPLN waveguide was found to be larger than that of a BBO (1.9 pm/V) [30] or

an LBO crystal (0.75 pm/V) [31] for the 399-nm SHG, but smaller than the typical coefficients of PPLN waveguides utilizing 1st-order quasi-phase matching ( $\sim 17$  pm/V) [39, 46]. It should be noted here that the nonlinear coefficient of 1st-order quasi-phase matching is theoretically three times larger than that of 3rd-order quasi-phase matching [44].

The conversion efficiency obtained with the present PPLN waveguide was less than that achieved with a power-buildup cavity. For example, a 399-nm power of up to 1.0 W has been demonstrated from a fundamental power of 1.3 W, with a conversion efficiency of 80%, using an LBO crystal in a cavity [31]. The conversion efficiency in the present experiment was limited by (a) the relatively small nonlinear coefficient  $d_{\text{eff}}$  (see above) and (b) the reduction of the SHG power for fundamental powers  $> 380$  mW, which is caused by the absorption of the light in the PPLN waveguide (see Sect. 3). The nonlinear coefficient can be increased by fabricating a poled structure with a short period (2.5  $\mu\text{m}$ ) needed for 1st-order quasi-phase matching. This fabrication is possible by using a high-voltage multi-pulse application method [47]. The reduction or the saturation of the SHG power for a high fundamental power has already been observed using PPLN waveguides for relatively short wavelengths [39, 48]. One possible way to reduce this effect is to fabricate a shorter waveguide. Such a waveguide provides a broader phase matching temperature acceptance [43], and thus relaxes the requirement of the temperature uniformity along the waveguide. However, the reduction of the waveguide length shortens the interaction length for SHG. There must be an optimum waveguide length that provides a sufficient interaction length and a broad temperature acceptance bandwidth.

For the laser cooling of Yb atoms, the obtained SHG power from the PPLN waveguide is needed to be amplified by injection locking. In a previous experiment [26], a seed power of 5 mW at 399 nm was used to amplify the laser power up to 220 mW. In the present experiment, we have already achieved a similar seed power (6 mW) with a good long-term stability. We have constructed a compact and robust light source at 399 nm that consists of an ECDL emitting at 798 nm with a tapered amplifier (TA) as a fundamental input laser, the present PPLN waveguide, and a slave diode laser for injection locking. In this laser system, active frequency stabilization is only needed for the 798-nm ECDL. One advantage of this laser system compared with an injection locked 399-nm slave diode laser using another blue ECDL is the utilization of a 798-nm diode laser which is useful for the reasons described in Sect. 1. Another advantage is that the 798-nm ECDL can easily be linked to an optical frequency comb based on a mode-locked erbium-doped fiber laser (1000 – 2050 nm) or a Ti:S laser (500 – 1100 nm). We have previously developed the fiber-based frequency combs for frequency stabilization of several light sources used in our Yb and Sr optical lattice clocks [49–51]. The 798-nm ECDL can similarly be stabilized to our frequency comb by detecting a heterodyne beat note between the 798-nm light and an SHG comb component. Figure 6 shows a picture of our 399-nm system developed on two breadboards with areas of 45 cm  $\times$  45 cm that can be installed in a transportable 19-inch rack. We constructed a Littrow-type ECDL operating at 798 nm using a red diode laser (Sanyo DL-LS2075). The 798-nm light from the ECDL was amplified by a TA (Eagleyard Photonics EYP-TPA-0808) and then coupled into the PPLN waveguide. The generated SHG light was coupled into a PM fiber and injected into a slave blue diode laser (Nichia NDV4B16) after passing through lenses for optimizing transverse mode matching between the seed and slave beams. The temperature of the slave diode laser was set at  $-4$   $^{\circ}\text{C}$  to adjust its output wavelength to 399 nm at the operation current of  $\sim 170$  mA. To prevent condensation, the slave diode laser was housed in a box which was purged with nitrogen. A small portion of the slave beam was sent to a scanning Fabry-Perot cavity (Thorlabs SA200-3B) for monitoring the longitudinal mode. The details of the other experimental parameters are described in [26]. Our laser system generated an output power of 200 mW at 399 nm when a seed power of 2 mW was injected into the slave laser. We successfully carried out laser cooling of Yb atoms using

